Published in final edited form as:

Cancer Res. 2019 May 15; 79(10): 2748–2760. doi:10.1158/0008-5472.CAN-18-2799.

An HK2 antisense oligonucleotide induces synthetic lethality in HK1^{-}HK2^{+} multiple myeloma

Shili Xu[1], **Tianyuan Zhou**[2], **Hanna M. Doh**[1], **K Ryan Trinh**[3], **Art Catapang**[1], **Jason T. Lee**[1,4,5], **Daniel Braas**[1,6], **Nicholas A. Bayley**[1], **Reiko E. Yamada**[7], **Alex Vasuthasawat**[3], **Joshua P. Sasine**[5,7], **John M. Timmerman**[5,7], **Sarah M. Larson**[5,7], **Youngsoo Kim**[2], **A. Robert MacLeod**[2], **Sherie L. Morrison**[3,5], and **Harvey R. Herschman**[1,4,5,8,9]

[1]Department of Molecular and Medical Pharmacology, David Geffen School of Medicine, University of California Los Angeles

[2]Ionis Pharmaceuticals Inc., Department of Antisense Drug Discovery, 2855 Gazelle Court, Carlsbad, CA 92010, USA

[3]Microbiology, Immunology & Molecular Genetics, David Geffen School of Medicine, University of California Los Angeles

[4]Crump Institute for Molecular Imaging, David Geffen School of Medicine, University of California Los Angeles

[5]Jonsson Comprehensive Cancer Center, David Geffen School of Medicine, University of California Los Angeles

[6]UCLA Metabolomics Center, David Geffen School of Medicine, University of California Los Angeles

[7]Department of Medicine, David Geffen School of Medicine, University of California Los Angeles

[8]Department of Biological Chemistry, David Geffen School of Medicine, University of California Los Angeles

[9]Molecular Biology Institute, David Geffen School of Medicine, University of California Los Angeles

Abstract

Although the majority of adult tissues express only hexokinase 1 (HK1) for glycolysis, most cancers express hexokinase 2 (HK2) and many co-express HK1 and HK2. In contrast to HK1^{+}HK2^{+} cancers, HK1^{-}HK2^{+} cancer subsets are sensitive to cytostasis induced by HK2^{shRNA} knockdown and are also sensitive to synthetic lethality in response to the combination of HK2^{shRNA} knockdown, an oxidative phosphorylation (OXPHOS) inhibitor diphenyleneiodonium (DPI), and a fatty acid oxidation (FAO) inhibitor perhexiline (PER). The majority of human multiple myeloma (MM) cell lines are HK1^{-}HK2^{+}. Here we describe an antisense oligonucleotide

Correspondence: Harvey R. Herschman. 341 Boyer Hall, UCLA, 611 Charles E. Young Drive East, Los Angeles, CA 90095. Phone: 310-825-8735. Fax: 310-825-1447. hherschman@mednet.ucla.edu.

Conflict of interest statement: T.Z, Y.K, and A.R.M are employees of IONIS Pharmaceuticals. Other authors declare that they have no conflict of interests.

(ASO) directed against human HK2 (HK2-ASO1), which suppressed HK2 expression in human MM cell cultures and human MM mouse xenograft models. The HK2-ASO1/DPI/PER triple-combination achieved synthetic lethality in MM cells in culture and prevented $HK1^{-}HK2^{+}$ MM tumor xenograft progression. DPI was replaceable by the FDA-approved OXPHOS inhibitor metformin (MET), both for synthetic lethality in culture and for inhibition of tumor xenograft progression. In addition, we used an ASO targeting murine HK2 (mHK2-ASO1) to validate the safety of mHK2-ASO1/MET/PER combination therapy in mice bearing murine MM tumors. HK2-ASO1 is the first agent that shows selective HK2 inhibition and therapeutic efficacy in cell culture and in animal models, supporting clinical development of this synthetically lethal combination as a therapy for $HK1^{-}HK2^{+}$ MM.

Introduction

Multiple myeloma (MM), a clonal proliferation disorder of malignant plasma cells, is the second most common hematologic malignancy. Despite application of currently available therapies (e.g. proteasome inhibitors, immunomodulatory drugs, tumor cell-targeting monoclonal antibodies, autologous stem cell transplantation), MM is still regarded as incurable (1); moreover, nearly all patients exhaust available therapeutic options, including clinical trials. The projected 60% increase in new MM cases between 2010 and 2030 highlights an urgent need for effective therapies (2).

Nearly all cancers exhibit increased glycolysis – originally described almost 90 years ago as the “Warburg effect” (3). Although suggested to provide adequate energy (ATP), reducing equivalents, and/or precursors for synthesizing building blocks for cancer cell survival and proliferation, the reason(s) for increased glycolysis in cancer cells is/are still ambiguous and controversial (4).

Despite many attempts to inhibit the increased glycolysis observed in cancers, no clinical therapy based on this approach has been successful, partially because of the conserved glycolytic pathways present in normal and cancer cells, and existence of alternative metabolic pathways in cancers (5). The first enzymatic step in glycolysis, conversion of glucose to glucose-6-phosphate, is catalyzed by members of the hexokinase (HK) family (6). Most tissues express only HK1; liver expresses only HK4 (also known as glucokinase). However, although HK2 is expressed in only a few normal tissues (e.g. heart, muscle, adipose tissue) and is expendable when globally deleted in adult mice (7), most tumors, regardless of tissue of origin, express HK2 in addition to HK1 (7–11).

In a search for cancers that depend primarily on HK2 expression, we observed that cancers from nearly all tissues have subsets of $HK1^{-}HK2^{+}$ tumors (11). $HK2^{shRNA}$ expression had no effect on cell proliferation or xenograft tumor progression for $HK1^{+}HK2^{+}$ tumors of differing origin; in contrast, $HK2^{shRNA}$ expression suppressed cultured cell proliferation and xenograft tumor progression of these $HK1^{-}HK2^{+}$ tumors (11).

Using both $HK1^{-}HK2^{+}$ and $HK1^{+}HK2^{+}$ liver cancer cell lines as well as $HK1^{-}HK2^{+}$ isogenic cancer cell lines derived from parental $HK1^{+}HK2^{+}$ cancer cells by CRISPR Cas9 deletion, a high throughput screen identified diphenyleneiodonium (DPI), a mitochondrial

complex I inhibitor, as a synergistic partner in inhibiting $HK1^{-}HK2^{+}$ tumor progression (12). Fatty acid oxidation (FAO) inhibition by the clinical drug perhexiline (PER) reduces ATP synthesis, and results in effective blockade of $HK1^{-}HK2^{+}$ tumor progression by the $HK2^{shRNA}$/DPI/PER combination. In contrast, $HK1^{+}HK2^{+}$ tumor progression was unaffected by this combination treatment (12).

Although $HK2^{shRNA}$ used in our previous studies lacks translational potential, it served as a valuable research tool to establish a proof-of-concept precision therapeutic strategy, using the $HK2^{shRNA}$/DPI/PER combination, for $HK1^{-}HK2^{+}$ liver cancer cells. However, the therapeutic challenges for this potential therapy include extending its efficacy to $HK1^{-}HK2^{+}$ cancer subsets from other tissues of origin, identifying a therapeutically tractable method to preferentially inhibit HK2, and finding appropriate clinical alternatives to inhibit ATP generation by OXPHOS.

In examining the Cancer Cell Line Encyclopedia (CCLE) dataset we found that MM has the highest percentage of $HK1^{-}HK2^{+}$ tumor subset members. Our objectives in this current study were four fold: (1) to extend our combination of inhibition of HK2 expression/activity, OXPHOS and FAO to $HK1^{-}HK2^{+}$ MM cancers, (2) to identify a potential clinically applicable therapeutic agent, as opposed to the research tool $HK2^{shRNA}$, to specifically suppress HK2 expression/activity, (3) to identify a more suitable clinical therapeutic alternative to inhibit OXPHOS and (4) to determine the tolerability of the combination by normal tissues in living animals. Here we used an HK2 antisense oligonucleotide (ASO), HK2-ASO1, to suppress human HK2 expression. Using human $HK1^{-}HK2^{+}$ MM cell lines as a model, we demonstrate that the HK2-ASO1/DPI/PER combination potently suppresses tumor progression. We also demonstrate that metformin (MET), an FDA-approved mitochondrial complex I inhibitor, can replace DPI in the synthetically lethal combination, improving the translational potential of the combination therapy. Finally, we used a mouse HK2 ASO to demonstrate, in $HK1^{-}HK2^{+}$ mouse MM tumor bearing mice, the efficacy and safety of the HK2-ASO/MET/PER combination therapy.

Materials and Methods

Cell Lines

Human MM cell lines OPM1, OPM2, RPMI8226, and XG1 from the American Type Culture Collection (ATCC) were cultured in Advanced RPMI1640+10% FBS. Human MM cell lines H929, U266, MM144, and S6B45 from ATCC were cultured in RPMI1640+10% FBS. Mouse MM P3X63Ag (P3) cells were cultured in IMDM+10% FBS. Cells were maintained at 37°C in 5% CO_2/95% air. Cell lines were used between passages 1 and 20, and were routinely authenticated based on morphology, growth characteristics, and HK expression profiles according to CCLE gene expression dataset. *Mycoplasma* contamination was routinely examined using MycoAlert (Lonza, #LT07–318).

ASOs

Gen 2.5 ASOs with constrained ethyl (cEt) chemistry were synthesized and used as described previously (13,14). Scrambled ASOs were included in each study as a negative

control. In cell culture, ASOs were delivered to the cells via free uptake, without using any transfecting agents. In animal studies, ASOs were dissolved in PBS and injected subcutaneously (s.c.).

Cell Proliferation Assay

Cell proliferation in 96-well plates was measured by CellTiter 96® AQ_{ueous} One Solution Assay (MTS) (Promega, #G5430) following the manufacturer's instructions.

Annexin V Apoptosis Assay

Cells were pre-treated with ASOs for three days before the addition of DPI, MET, or PER. Three days later, cells were harvested, washed, and stained using the Vybrant Apoptosis Kit (ThermoFisher, Waltham, MA) according to the manufacturer's protocol. Stained samples were then examined on a Becton Dickenson FACSVerse flow cytometer and analyzed using FlowJo software.

Assessment of Xenograft MM Progression

In subcutaneous (s.c.) models, 3×10^6 cells suspended in 100 μL RPMI/Matrigel (1:1) were implanted subcutaneously in NSG mice under aseptic conditions. MM progression was assessed by biweekly measurement of tumor diameters with a Vernier caliper. Tumor volume (mm^3) was calculated as $= D \times d^2/2$, where D and d are the longest and shortest tumor diameters. Treatments started when tumors reached 200 mm^3. In disseminated MM models, 1×10^6 P3/HK1$^-$-mCherry-LUC cells or 3×10^6 RPMI8226-LUC cells suspended in 100 μL PBS were injected intravenously (i.v.). MM progression was monitored once weekly by bioluminescence imaging (BLI). Treatments started when tumors were detected by BLI. To test our treatments, mice were randomized into indicated treatment groups to receive daily treatment for 5 days per week, with 2-day breaks between weeks. ASOs were given by subcutaneous injection at 50 mg/kg. DPI and PER were dissolved in DMSO as stock solutions at 30 mg/ml and 300 mg/ml, respectively, and then diluted in 5% (w/v) hydroxyl-propyl-beta-cyclodextrin (Sigma). MET was dissolved in 5% (w/v) hydroxyl-propyl-beta-cyclodextrin. All solutions for injection were filtered. DPI, PER, and MET were given at 2 mg/kg, 30 mg/kg, and 250 mg/kg through intraperitoneal (i.p.) injection. All reported animal studies were approved by the UCLA Chancellor's Animal Research Committee (ARC) under protocol number 2015-067-11.

In Vivo Assessment of Tumor Glucose Consumption by ^{18}F-FDG PET/CT.

Animals without fasting were warmed on a heating pad for 30 min and then injected via the tail vein with 2.8 MBq of clinical-grade ^{18}F-fluorodeoxyglucose (^{18}F-FDG). Animals underwent a 1 hr conscious ^{18}F-FDG biodistribution period on a heating pad prior to imaging. Positron emission tomography (PET) and computed tomography (CT) scans were conducted on a G8 combined PET/CT instrument (Sofie Biosciences, Inc.) with a 600-s PET acquisition and maximum-likelihood expectation maximization reconstruction, and with a 50-s CT acquisition and Feldkamp reconstruction. PET data were converted to percent-injected dose per gram (%ID/g) and PET/CT images were co-registered. Mean values of

PET signal intensity from tumor region-of-interest (ROI) were analyzed using AMIDE software v1.0.4.

Statistical Analysis

The Student's t-test was used for statistical analysis. *P* values were determined using Prism 5 (GraphPad Software, Inc.). Differences were considered statistically significant at $P < 0.05$.

Results

A substantial subset of MM cell lines does not express HK1

Analysis of HK1 and HK2 mRNA expression in the Cancer Cell Line Encyclopedia (CCLE) database revealed that 54% of the human MM cell lines in this collection are $HK1^{-}HK2^{+}$ (Figs. 1A, 1B). Among all human cancer types in the CCLE, MM has the largest percentage of $HK1^{-}HK2^{+}$ cell lines (54%; 14/26), followed by liver cancer (38%; 9/24) and colorectal cancer (10 %; 6/58) (Fig. 1B). Existence of the $HK1^{-}HK2^{+}$ characteristic in many MM cell lines was confirmed at the protein level (Fig. 1C).

To consider HK1 and HK2 expression in MM clinical samples, we analyzed HK1 and HK2 mRNA expression profiles in the MM patient samples from the Relating Clinical Outcomes in MM to Personal Assessment of Genetic Profile (CoMMpass) data base (https://research.themmrf.org) (15,16), and compared them to those of the MM cell lines in the CCLE data base. Although the absolute levels of HK1 and HK2 mRNAs between the CCLE data base and the CoMMpass data base cannot be directly compared, due to differences in sequencing methods and approaches, the relative levels of expression can be compared. We defined the frequency of "low" expression of HK1 in MM cell lines (data from the CCLE data set), and identified the equivalent proportion of the MMs in the patient population (data from the CoMMpass data base) (Fig. 1D). We then compared HK2 mRNA levels in the "HK1 low" sub-populations from the two data bases. HK2 expression in the "HK1 low" and "HK1 high" sub-populations are the same in MM CCLE and CoMMpass data base members (Fig. 1D), indicating a similar high frequency of the $HK1^{-}HK2^{+}$ phenotype in clinical MM patient samples.

Differential gene expression analysis of all MM cell lines in the CCLE dataset reveals distinct gene expression patterns between the $HK1^{-}HK2^{+}$ and the $HK1^{+}HK2^{+}$ MM cell lines, further supporting classification of the $HK1^{-}HK2^{+}$ MMs and the $HK1^{+}HK2^{+}$ MMs as distinct subtypes (Fig. 1E). Pathway enrichment analysis suggests that these differentially expressed genes are involved in pathways that include endocytosis, N-glycan biosynthesis, glycosphingolipid biosynthesis, galactose metabolism, homologous recombination, regulation of actin cytoskeleton, fructose and mannose metabolism, and amino sugar and nucleotide sugar metabolism (Fig. 1F). These data may suggest additional potential biomarkers and/or therapeutic targets for the $HK1^{-}HK2^{+}$ and $HK1^{+}HK2^{+}$ MM subtypes.

Development of an HK2 ASO to suppress HK2 expression and HK1^{-}HK2^{+} MM cell proliferation.

Extensive efforts have been made to develop HK2 specific small-molecule inhibitors (17), but no specific HK2 inhibitor has been reported to exhibit *in vivo* systemic efficacy. To translate our previous findings, using genetic approaches, that HK2 is targetable to slow the progression of HK1^{-}HK2^{+} subsets of cancer, we used our latest Generation 2.5 Chemistry technology to make HK2 ASOs as pharmacologic HK2-targeting agents to treat HK1^{-}HK2^{+} MMs. We identified two active HK2 ASOs (HK2-ASO1 and HK2-ASO2) (Fig. S1A) after *in vitro* screening and tolerability study in mice. In cell culture, delivered via free uptake without using any transfecting agents, HK2-ASO1 was more effective than HK2-ASO2 in suppressing HK2 expression, in a dose-dependent manner, in a broad panel of MM cell lines of both the HK1^{-}HK2^{+} and the HK1^{+}HK2^{+} subtypes, without altering HK1 protein levels (Fig. 2A).

Glucose consumption and lactate production are metabolic markers of HK enzymatic activity in driving glycolysis. Treatment with HK2-ASO1 reduced both glucose consumption and lactate production (Fig. 2B). However, although HK2-ASO1 and HK2-ASO2 suppressed HK2 expression in both HK1^{-}HK2^{+} and HK1^{+}HK2^{+} MM cell lines, both ASOs only reduced proliferation of MM cells with the HK1^{-}HK2^{+} characteristic (Fig. 2C); they had no significant effect on HK1^{+}HK2^{+} MM cell proliferation (Fig. 2C), despite comparable HK2 knockdown in all cell lines. Cell cycle analyses showed that HK2-ASO1, compared to a control ASO (ASO-Ctrl), significantly decreased S phase proliferating cell population in HK1^{-}HK2^{+} MM cells, but not in HK1^{+}HK2^{+} MM cells (Fig. S1B). In addition, HK2-ASO1 had only minor effect on increasing MM cell death, as indicated by the < 10% sub-G1 cell population (Fig. S1C).

The selective growth inhibitory effect of HK2-ASO1 in HK1^{-}HK2^{+} MM cells in cell culture was validated both by cell counting (Fig. S1D) and by colony formation assays (Fig. S1E), compared with ASO-Ctrl. These observations with ASO HK2-selective inhibitors are consistent with our previous findings with other cancer cells using HK2^{shRNA} (11,12), demonstrating that the cytostatic effect of HK2 knockdown or knockout is limited to the HK1^{-}HK2^{+} cancer subsets.

The combination of HK2-ASO1, partial inhibition of OXPHOS, and FAO is synthetically lethal for HK1^{-}HK2^{+} MMs.

We previously identified a small-molecule mitochondrial complex I inhibitor, DPI, from a high throughput screen as a synthetically lethal partner with HK2 shRNAs in HK1^{-}HK2^{+} liver cancer cells (12). At concentrations (< 100 nM) we used in our subsequent cell culture experiments DPI partially, but not completely, inhibited mitochondrial OXPHOS (Fig. S2A). The synthetic lethality of the HK2^{shRNA} + DPI combination could be enhanced by the addition of the FAO inhibitor perhexiline (PER) (12). Consistent with our previous observations with HK2 shRNAs, the combination of HK2-ASO1 and DPI induced synthetic lethality in HK1^{-}HK2^{+} MM cell lines, but had no discernable effect on viability or proliferation of HK1^{+}HK2^{+} U266 MM cells (Fig. 3A, Fig. S2B). Apoptosis induction by the HK2-ASO1/DPI combination was also observed only in HK1^{-}HK2^{+} MM cell lines, but not

in $HK1^{+}HK2^{+}$ MM cells (Fig. 3B). To test the sensitizing effect of PER (12), we lowered HK2-ASO1 and DPI concentrations so that the HK2-ASO1/DPI combination did not induce substantial apoptosis in $HK1^{+}HK2^{+}$ OPM2 MM cells (Fig. 3C). Addition of PER sensitized these $HK1^{-}HK2^{+}$ MM cells to this HK2-ASO1/DPI combination (Fig. 3C, Fig.S2C). Targeting the major bioenergy generation pathways in $HK1^{-}HK2^{+}$ MM cell lines (HK2-driven glycolysis and OXPHOS) with HK2-ASO1 and DPI triggered expression of an apoptosis marker, cleaved PARP. Addition of PER to the HK2-ASO1+ DPI combination further increased PARP cleavage (Fig. 3D).

We also examined the effect of this triple combination on human peripheral blood mononuclear cells (PBMCs). Compared to $HK1^{+}HK2^{+}$ MM OCI-My5 cells, PBMCs have high HK1 expression and low HK2 expression (Fig. 3E). Although HK2-ASO1 reduced HK2 levels in PBMCs (Fig. 3E), the combination of HK2-ASO1/DPI/PER had no significant toxicity in PBMCs (Fig. 3F), suggesting its potential safety for *in vivo* utility.

To further evaluate the specificity of our combination therapy for $HK1^{-}HK2^{+}$ MM cells, we created an $HK1^{+}HK2^{+}$ isogenic cell line (RPMI8226/$HK1^{+}HK2^{+}$) from the parental $HK1^{-}HK2^{+}$ RPMI8226 cell line (Fig. 3G). Stable expression of HK1 resulted in acquired resistance of RPMI8226 ($HK1^{-}HK2^{+}$) cells to the cytotoxicity of the HK2-ASO1/DPI/PER combination in this isogenic cell line experiment (Fig. 3H), confirming the specificity of the synthetic lethality in $HK1^{-}HK2^{+}$ MM cells.

HK2-ASO1 reduces HK2 expression and ^{18}F-FDG accumulation in xenograft MM tumors *in vivo*.

We next examined the ability of HK2-ASO1 to suppress HK2 expression in human MM tumors in mouse xenografts. Subcutaneous (s.c.) injection of HK2-ASO1 effectively reduced HK2 protein levels in both xenograft $HK1^{-}HK2^{+}$ OPM2 tumors and $HK1^{+}HK2^{+}$ U266 tumors, without affecting HK1 expression (Fig. 4A). To demonstrate the biochemical consequences of HK2-ASO1-suppressed HK2 expression in human $HK1^{-}HK2^{+}$ MM tumors *in vivo*, we examined ^{18}F-FDG accumulation in $HK1^{-}HK2^{+}$ OPM2 MM xenograft tumors, by ^{18}F-FDG microPET analysis, in the presence of HK2-ASO1 or ASO-Ctrl. Decrease in HK2 protein levels by HK2-ASO1 (Fig. 4A) significantly reduced OPM2 tumor ^{18}F-FDG accumulation, as determined non-invasively by ^{18}F-FDG PET imaging (Figs. 4B and 4C).

HK2-ASO1 synergizes with DPI and PER to suppress $HK1^{-}HK2^{+}$ xenograft human MM tumor progression.

We previously demonstrated the efficacy of $HK2^{shRNA}$-mediated suppression of HK2 expression in a therapeutic combination with DPI and PER for $HK1^{-}HK2^{+}$ liver cancer tumor progression (12). Here we tested HK2-ASO1 efficacy, alone and in combination with DPI and PER, on $HK1^{-}HK2^{+}$ MM xenograft tumor progression. HK2-ASO1 treatment was started when s.c. OPM2 $HK1^{-}HK2^{+}$ MM tumors reached 200 mm^3 (day 1); DPI and PER treatments were initiated on day 4. As a single agent, HK2-ASO1 did not reduce OPM2 tumor progression to a statistically significant level (Fig. 4D). However, the HK2-ASO1/DPI combination significantly suppressed tumor progression, and addition of PER resulted in a further reduction in tumor volume (Fig. 4D). HK2-ASO1, both alone and in combination

with DPI/PER, is tolerated by the animals; no significant change in body weight was detected among the experimental groups (Fig. S3A). However, it is important to note that HK2-ASO1 is specific for human HK2 and does not match the mouse HK2 sequence. Therefore, tolerability of human HK2-targeting HK2-ASO1 in xenograft experiments does not indicate tolerability of HK2 silencing in the triple combination in normally HK2 expressing tissues (e.g. heart and skeletal muscle).

At the end of the experiment, tumors were collected (Fig. S3B) and weighed (Fig. S3C). Significant reductions in both tumor volume and weight occurred. In contrast, DPI and PER, as single agents or in combination, did not significantly affect OPM2 tumor progression (Figs. S3D and S3E). In both the HK2-ASO1/DPI group and the HK2-ASO1/DPI/PER group, increase in PARP cleavage was detected in tumor homogenates of OPM2 $HK1^{-}HK2^{+}$ MM tumors (Fig. 4E).

Unlike the $HK1^{-}HK2^{+}$ OPM2 tumors, $HK1^{+}HK2^{+}$ U266 MM tumors were resistant to treatments with HK2-ASO1, HK2-ASO1/DPI and HK2-ASO1/DPI/PER (Fig. 4F). No significant difference was observed in tumor volume (Fig. S3F) or tumor weight (Fig. S3G), although HK2 protein levels were substantially reduced in tumors (Fig. S3H). These *in vivo* data confirm that HK2-ASO1/DPI/PER combination therapy is effective in suppressing $HK1^{-}HK2^{+}$ MM tumor xenograft progression, but has no significant effect on $HK1^{+}HK2^{+}$ MM tumor xenograft progression.

DPI can be replaced by metformin (MET) in this combination therapy.

Our data suggest that ASOs that suppress HK2 expression are a potential clinical therapeutic approach to treating $HK1^{-}HK2^{+}$ MM. Although DPI is a potent OXPHOS inhibitor and has been demonstrated to synergize therapeutically with $HK2^{shRNA}$ (12) and HK2-ASO1, DPI has not been tested in humans. To move this combination therapy towards clinical development, we tested the replacement of DPI with the FDA approved OXPHOS inhibitor metformin (MET). Like DPI, MET partially inhibited mitochondrial respiration (Fig. S4A), and demonstrated synthetic lethality with HK2-ASO1 in cultured $HK1^{-}HK2^{+}$ MM cells, but had no significant effect on $HK1^{+}HK2^{+}$ U266 MM cells (Fig. 5A, Fig. S4B). The HK2-ASO1/MET combination triggered apoptosis in $HK1^{-}HK2^{+}$ MM cells (Fig. 5B), and the apoptotic effect was enhanced by PER (Fig. 5C and Fig. S4C).

Multiple myeloma tumors are found in the bone (1), an environment proposed to protect the tumor cells from therapeutic agents (18). Using culture conditions, we next examined the effect of bone marrow microenvironment interactions on the efficacy of our HK2-ASO1/MET/PER triple combination therapy. Cocultures of luciferase (LUC) expressing $HK1^{-}HK2^{+}$ RPMI8226 MM cells with human bone marrow stromal cells (BMSCs), using a 1:2 ratio of MM cells to BMSCs (19), did not affect the cytotoxicity of our triple combination therapy, although the presence of BMSCs lowered the sensitivity of RPMI8226 cells to HK2-ASO1 as a single agent (Fig. 5D and 5E).

The *in vivo* activity of OXPHOS inhibitors can be non-invasively monitored by ^{18}F-FDG PET, because OXPHOS inhibition forces cells to up-regulate glycolytic activity to compensate loss in energy production, resulting in an increase in ^{18}F-FDG PET signal. MET

and DPI treatments comparably increased ^{18}F-FDG accumulation in HK1^{-}HK2^{+} OPM2 MM tumors (Fig. S4D).

While MET alone did not significantly affect OPM2 tumor progression (Fig. 5F), the HK2-ASO1/MET/PER combination was comparable to the HK2-ASO1/DPI/PER combination both in suppression of s.c. HK1^{-}HK2^{+} tumor progression (Fig. 5F) and in PARP cleavage induction (Fig. S4E). These results support replacing DPI with MET to translate this combination therapy into a precision medicine therapy alternative to treat patients with HK1^{-}HK2^{+} MM.

MM is a systemic hematopoietic disease. To examine the efficacy of the triple therapy on systemic MM progression, we used a previously validated systemic MM model with human HK1^{-}HK2^{+} RPMI8226/LUC cells (19). Following intravenous (i.v.) injection of MM cells, cohorts of mice were treated either with ASO-Ctrl or with the HK2-ASO1/MET/PER combination therapy, and disease progression was monitored by bioluminescence imaging (BLI) at the times indicated in Fig. 5G. As observed for s.c. human HK1^{-}HK2^{+} OPM2 tumors (Fig. 5F), systemic HK1^{-}HK2^{+} RPMI8226/LUC tumor progression was dramatically reduced by the triple combination (Fig. 5G and 5H).

HK2-ASO1/DPI/PER and HK2-ASO1/MET/PER combination therapies have similar impacts on HK1^{-}HK2^{+} MM cell metabolism.

By targeting OXPHOS, both DPI and MET increased glycolysis in OPM2 cells, while HK2-ASO1 blocked HK2-driven glycolysis (Fig. 6A). Consistent with these observations, co-inhibition of HK2-driven glycolysis and OXPHOS reduced cellular ATP/(AMP+ADP) ratios more than single pathway inhibition. Although FAO inhibition alone by PER has no significant effect on the ATP/(AMP+ADP) ratio, FAO inhibition reduced the ATP/(AMP +ADP) ratios in HK1^{-}HK2^{+} OPM2 cells exposed both to HK2-ASO1+DPI and to HK2-ASO1+MET (Fig. 6B). These metabolic changes occurred prior to cell death (Fig. 6C).

Global metabolic profiling demonstrated that MET and DPI, as single agents, exert essentially identical effects on cell metabolism (Fig. 6D). The combinations of HK2-ASO1+DPI+PER and HK2-ASO1+MET+PER share similar patterns of metabolic alterations, distinct from metabolic alterations elicited by the single-agents (Fig. 6D). In particular, the triple-combinations (HK2-ASO1+DPI+PER and HK2-ASO1+MET+PER) substantially decreased the intracellular pool sizes of many amino acids, nearly all metabolites in the TCA cycle, some fatty acid intermediates, and all metabolites in purine and pyrimidine biosynthesis (Fig. 6E, Fig. S5, and Table S1). The triple-combination therapies substantially altered the global metabolism of HK1^{-}HK2^{+} MM cells, likely contributing to the synthetic lethality.

Using [U-^{13}C]-glucose as a carbon source to label metabolites *de novo* synthesized, we further observed that the ^{13}C-labeled portions of many amino acids, metabolites in the TCA cycle and nucleotide biosynthesis were substantially decreased by the triple-combinations (Fig. 6F, and Fig. S6). Taken together, our results indicate that the triple-combinations HK2-ASO1/MET/PER and HK2-ASO1/DPI/PER induce global metabolic alterations similar to one another, and distinct from those elicited by single agents; the triple-combinations reduce

both the pool sizes of many key metabolites and their *de novo*, glucose-dependent biosynthesis.

HK2-ASO/DPI/PER and HK2-ASO/MET/PER combinations are tolerated by normal tissues.

While the triple-combinations using HK2-ASO1 show efficacy in suppressing human $HK1^{-}HK2^{+}$ MM tumor progression in xenograft models (Fig. 5F, 5G and 5H), it remained unclear whether mice can tolerate the triple-combination with HK2 inhibition in normal tissues; the mRNAs for mouse and human HK2 differ in sequence and are, consequently, likely to differ in inhibition by ASOs directed against HK2 from the alternative species. To address this question, two ASOs, mHK2-ASO1 and mHK2-ASO2 (Fig. S7A) were developed to be tested in HK2-ASO/DPI/PER and HK2-ASO/MET/PER triple-combinations in mice bearing mouse $HK1^{-}HK2^{+}$ MMs. As anticipated, HK2-ASO1 targets human HK2 but not mouse HK2 (Fig. S7B).

mHK2-ASO1 and mHK2-ASO2 suppressed mouse HK2 expression in mouse MM P3X63Ag (P3) cells (20) without affecting HK1 expression (Fig. S7C). To model human $HK1^{-}HK2^{+}$ MMs, isogenic $HK1^{-}HK2^{+}$ mouse P3 cells were generated using CRISPR-Cas9 deletion (Fig. S7D). Both mHK2-ASO1 and mHK2-ASO2 suppressed HK2 expression to equivalent degrees in the parental P3 cells and in the P3 $HK1^{KO}$ cells (Fig. 7A and Fig. S7C). While ASO-mediated HK2 knockdown did not affect proliferation of parental $HK1^{+}HK2^{+}$ P3 cells in culture, both mHK2-ASO1 and mHK2-ASO2 inhibited proliferation of the isogenic $HK1^{-}HK2^{+}$ P3/$HK1^{KO}$ cells (Fig. S7E). mHK2-ASO1/DPI/PER and mHK2-ASO1/MET/PER triple-combinations induced similar synthetic lethality responses in cultured $HK1^{-}HK2^{+}$ P3 $HK1^{KO}$ cells (Fig. 7B).

In mice bearing s.c. isogenic $HK1^{-}HK2^{+}$ and $HK1^{+}HK2^{+}$ P3 tumors, mHK2-ASO1 and mHK2-ASO2 both reduced HK2 levels in tumors and to a lesser extent in the heart (Fig. S7F). In contrast, neither mHK2-ASO1 nor mHK2-ASO2 affected HK2 expression in skeletal muscle (Fig. S7F). As expected, neither mHK2-ASO1 nor mHK2-ASO2 affected HK1 expression (Fig. S7F). ^{18}F-FDG PET scans demonstrated significantly decreased ^{18}F-FDG accumulation in s.c. $HK1^{-}HK2^{+}$ P3 tumors after mHK2-ASO1, mHK2-ASO1/MET/PER, or mHK2-ASO1/DPI/PER treatments (Fig. 7C). mHK2-ASO1 alone significantly reduced $HK1^{-}HK2^{+}$ P3 tumor progression (Fig. 7D). Moreover, mHK2-ASO1/MET/PER and mHK2-ASO1/DPI/PER substantially and equivalently decreased s.c. $HK1^{-}HK2^{+}$ P3 tumor progression compared to mHK2-ASO1 alone (Fig. 7D). At the experiment endpoint, tumors were collected (Fig. S7G), weighed (Fig. S7H), and analyzed for HK2 expression (Fig. S7I). Both mHK2-ASO1/MET/PER and mHK2-ASO1/DPI/PER triple-combinations were tolerated by the mice as indicated by body weight (Fig. 7E). These data suggest that the HK2 ASO+MET+PER combination is likely to be tolerated for human $HK1^{-}HK2^{+}$ MM therapy.

We also established a disseminated mouse MM model, using i.v. injected P3 $HK1^{-}HK2^{+}$ cells expressing both LUC (for BLI imaging) and mCherry (for fluorescent quantification of MM cells in bone marrow extracts). Bone marrow extraction on day 18 post-injection identified 27.2 ± 4.2% of the cells as mCherry-labeled MM cells (Fig. S7J). The mHK2-ASO1/MET/PER combination significantly suppressed the progression of this highly

aggressive disseminated mouse MM model, as determined by BLI (Figs. 7F and G). The experiment was terminated following euthanization of the last control mouse; all treated mice were alive and appeared healthy at the end of the experiment (Fig. 7H). These data demonstrate, in the mouse systemic model, that the triple-combination shows efficacy in suppressing $HK1^{-}HK2^{+}$ MM tumor progression and is tolerated by normal tissues.

Discussion

It is only relatively recently that HK2 expression has been recognized as a common feature of many cancers (7,8,10,21). Because HK2 is not expressed in most normal tissues, targeting HK2 has become a popular goal as an approach to cancer management. In the absence of systemically effective selective HK2 inhibitors, several laboratories, using HK2-targeted shRNAs, reported success in retarding, reducing, or eliminating $HK1^{+}HK2^{+}$ xenograft tumor progression (7,8,10,21). However, when this question was reexamined, both with alternative HK2 shRNAs and with isogenic $HK1^{-}$ $HK2^{+}$ and $HK1^{+}HK2^{+}$ cancer cell line pairs created by CRISPR Cas9 deletion, it became clear that HK1 and HK2 can compensate each other; either is sufficient to support cancer cell proliferation in culture and for xenograft tumor progression *in vivo* (11). Consistent with these observations, neither HK2 nor HK1 were identified as essential genes for cell proliferation in an unbiased systematic CRISPR Cas9 screen of $HK1^{+}HK2^{+}$ cancer cell lines (22). In contrast, however, HK2 shRNA expression was cytostatic for $HK1^{-}HK2^{+}$ cancer cells, and reduced, but did not eliminate, $HK1^{-}HK2^{+}$ xenograft tumor progression *in vivo* (12).

In examining the HK isoform expression of human cancer cell lines in the CCLE collection it became clear that liver cancers and MMs have the greatest percentages of $HK1^{-}HK2^{+}$ cell lines. Because examination of the TCGA data base revealed that primary liver cancer specimens are enriched in $HK1^{-}HK2^{+}$ samples, we turned first to these tumors to develop an effective experimental therapy for $HK1^{-}HK2^{+}$ tumors that incorporates elimination of HK2 activity. We demonstrated that combined $HK2^{shRNA}$ knockdown and mitochondrial complex I inhibition achieves synthetic lethality in $HK1^{-}HK2^{+}$ liver cancer cells, and determined that FAO inhibition by PER, in combination with $HK2^{shRNA}$ knockdown and OXPHOS inhibition, prevented liver $HK1^{-}HK2^{+}$ tumor xenograft progression (12).

In this current study our goals were to determine whether $HK1^{-}HK2^{+}$ MMs were also susceptible to synthetic lethality mediated by inhibition of HK2 expression, OXPHOS and FAO, and to identify inhibitory agents for each component that are more appropriate for clinical application. Despite substantial attempts (17), no systemically efficacious targeted HK2 inhibitor has been reported. To move the $HK2^{shRNA}$/DPI/PER combination therapy described previously (12) toward treatment for $HK1^{-}HK2^{+}$ MMs, we replaced HK2 shRNA with HK2-ASO1 to reduce HK2 expression. To our knowledge, HK2-ASO1 is the first pharmaceutical agent with a systemic *in vivo* ability to reduce HK2 activity, with little or no effect on HK1 activity, in tumors.

A significant advantage of ASOs relative to traditional small molecule-based drugs is their exquisite target specificity. Metabolic reprogramming in cancer frequently results from metabolic enzyme isoform switches (12,23–25). The mRNA sequences of these cancer-

specific isoforms can be exploited to target cancer cells, with minimal effects on normal tissues that express different enzyme isoforms. Due to the extensive similarities in protein structures and substrate binding sites between these enzyme isoforms, targeting the cancer specific isoforms by ASOs to exploit isoform-specific differences in mRNA sequences provides a promising therapeutic strategy.

Again, to employ more clinically relevant agents for the HK2i/OXPHOSi/FAOi combination therapy, we replaced the potent mitochondrial complex I inhibitor DPI (12) with an FDA-approved inhibitor, MET. MET can replace DPI in proliferation and viability studies, global metabolomics analyses, ^{18}F-FDG/microPET imaging and tumor xenograft progression. PER is in clinical use as an antianginal drug in Asia and Australia, and in phase 2/3 clinical trials in the US.

Tumor cell expression of shRNAs targeting human HK2 in xenograft models (7,8,10,21) cannot properly evaluate adverse effects of HK2 inhibition in normal tissues; because of differences in human and mouse HK2 mRNA sequences, ASOs that target human HK2 have no effect on mouse HK2 expression (Fig. S7B). However, using a mouse MM tumor/host model, the mouse HK2-ASOs/MET/PER therapeutic combination exhibits both potency and safety, suggesting that HK2-ASO1/MET/PER could be tolerated by normal tissues in patients. Consequently, an HK2-ASO/MET/PER combination could be a promising translational precision medicine therapy for $HK1^{-}HK2^{+}$ MMs. Additional studies need be done to further identify HK2-ASOs suitable for clinical investigation. In addition, the clinical potential of our observations can be further validated by future experiments that employ primary patient-derived $HK1^{-}HK2^{+}$ MM cells and patient-derived xenograft models of $HK1^{-}HK2^{+}$ MMs.

Stratification of MM patients to identify those individuals whose tumors are $HK1^{-}HK2^{+}$ would be required for the clinical success of this precision medicine therapy. Due to HK1 expression in most normal tissues, and consequent contamination with non-cancer HK1-expressing cells in tumor biopsies, single-cell analyses with MM marker staining (e.g. CD138, BCMA) are likely to be required for patient stratification. In addition to MM, other cancers also have $HK1^{-}HK2^{+}$ subsets (11). These $HK1^{-}HK2^{+}$ cancers are also susceptible to HK2 inhibition, regardless of their tissues of origin (11). Therefore, in combination with patient stratification strategies, an HK2-ASO/MET/PER combination has potential as a precision medicine therapy to treat $HK1^{-}HK2^{+}$ tumors, regardless of their tissue of origin.

Supplementary Material

Refer to Web version on PubMed Central for supplementary material.

Acknowledgments

The project is supported by the JCCC/CTSI/DGSOM Cancer Theme Impact Grant (Grant No: UL1TR001881). HRH is supported by the Phelps Family Foundation and the Crump Family Foundation. SLM is supported by NIH R01 CA200910.

Abbreviations:

ASO	antisense oligonucleotide
DPI	diphenyleneiodonium
FAO	fatty acid oxidation
FDG	fluorodeoxyglucose
HK	hexokinase
MET	metformin
MM	multiple myeloma
OXPHOS	oxidative phosphorylation
PER	perhexiline
PET	positron emission tomography

References

1. Kumar SK, Rajkumar V, Kyle RA, van Duin M, Sonneveld P, Mateos MV, et al. Multiple myeloma. Nat Rev Dis Primers 2017;3:17046 [PubMed: 28726797]
2. Smith BD, Smith GL, Hurria A, Hortobagyi GN, Buchholz TA. Future of cancer incidence in the United States: burdens upon an aging, changing nation. J Clin Oncol 2009;27:2758–65 [PubMed: 19403886]
3. Schulze A, Harris AL. How cancer metabolism is tuned for proliferation and vulnerable to disruption. Nature 2012;491:364–73 [PubMed: 23151579]
4. Liberti MV, Locasale JW. The Warburg Effect: How Does it Benefit Cancer Cells? Trends Biochem Sci 2016;41:211–8 [PubMed: 26778478]
5. Pelicano H, Martin DS, Xu RH, Huang P. Glycolysis inhibition for anticancer treatment. Oncogene 2006;25:4633–46 [PubMed: 16892078]
6. Wilson JE. Isozymes of mammalian hexokinase: structure, subcellular localization and metabolic function. J Exp Biol 2003;206:2049–57 [PubMed: 12756287]
7. Patra KC, Wang Q, Bhaskar PT, Miller L, Wang Z, Wheaton W, et al. Hexokinase 2 is required for tumor initiation and maintenance and its systemic deletion is therapeutic in mouse models of cancer. Cancer Cell 2013;24:213–28 [PubMed: 23911236]
8. Wang L, Xiong H, Wu F, Zhang Y, Wang J, Zhao L, et al. Hexokinase 2-mediated Warburg effect is required for PTEN- and p53-deficiency-driven prostate cancer growth. Cell Rep 2014;8:1461–74 [PubMed: 25176644]
9. Cea M, Cagnetta A, Acharya C, Acharya P, Tai YT, Yang C, et al. Dual NAMPT and BTK targeting leads to synergistic killing of Waldenstrom Macroglobulinemia cells regardless of MYD88 and CXCR4 somatic mutation status. Clin Cancer Res 2016;22:6099–109 [PubMed: 27287071]
10. Wolf A, Agnihotri S, Micallef J, Mukherjee J, Sabha N, Cairns R, et al. Hexokinase 2 is a key mediator of aerobic glycolysis and promotes tumor growth in human glioblastoma multiforme. J Exp Med 2011;208:313–26 [PubMed: 21242296]
11. Xu S, Catapang A, Doh HM, Bayley NA, Lee JT, Braas D, et al. Hexokinase 2 is targetable for HK1 negative, HK2 positive tumors from a wide variety of tissues of origin. J Nucl Med 2018
12. Xu S, Catapang A, Braas D, Stiles L, Doh HM, Lee JT, et al. A precision therapeutic strategy for hexokinase 1-null, hexokinase 2-positive cancers. Cancer Metab 2018;6:7 [PubMed: 29988332]

13. Seth PP, Siwkowski A, Allerson CR, Vasquez G, Lee S, Prakash TP, et al. Short antisense oligonucleotides with novel 2'−4' conformationaly restricted nucleoside analogues show improved potency without increased toxicity in animals. J Med Chem 2009;52:10–3 [PubMed: 19086780]
14. Hong D, Kurzrock R, Kim Y, Woessner R, Younes A, Nemunaitis J, et al. AZD9150, a next-generation antisense oligonucleotide inhibitor of STAT3 with early evidence of clinical activity in lymphoma and lung cancer. Sci Transl Med 2015;7:314ra185
15. Lazzari E, Mondala PK, Santos ND, Miller AC, Pineda G, Jiang Q, et al. Alu-dependent RNA editing of GLI1 promotes malignant regeneration in multiple myeloma. Nat Commun 2017;8:1922 [PubMed: 29203771]
16. Manojlovic Z, Christofferson A, Liang WS, Aldrich J, Washington M, Wong S, et al. Comprehensive molecular profiling of 718 Multiple Myelomas reveals significant differences in mutation frequencies between African and European descent cases. PLoS Genet 2017;13:e1007087 [PubMed: 29166413]
17. Lin H, Zeng J, Xie R, Schulz MJ, Tedesco R, Qu J, et al. Discovery of a novel 2,6-disubstituted glucosamine series of potent and selective hexokinase 2 inhibitors. ACS Med Chem Lett 2016;7:217–22 [PubMed: 26985301]
18. Di Marzo L, Desantis V, Solimando AG, Ruggieri S, Annese T, Nico B, et al. Microenvironment drug resistance in multiple myeloma: emerging new players. Oncotarget 2016;7:60698–711 [PubMed: 27474171]
19. Sherbenou DW, Aftab BT, Su Y, Behrens CR, Wiita A, Logan AC, et al. Antibody-drug conjugate targeting CD46 eliminates multiple myeloma cells. J Clin Invest 2016;126:4640–53 [PubMed: 27841764]
20. Malouf NN, Coronado R, McMahon D, Meissner G, Gillespie GY. Monoclonal antibody specific for the transverse tubular membrane of skeletal muscle activates the dihydropyridine-sensitive Ca2+ channel. Proc Natl Acad Sci U S A 1987;84:5019–23 [PubMed: 2440040]
21. Anderson M, Marayati R, Moffitt R, Yeh JJ. Hexokinase 2 promotes tumor growth and metastasis by regulating lactate production in pancreatic cancer. Oncotarget 2017;8:56081–94 [PubMed: 28915575]
22. Wang T, Birsoy K, Hughes NW, Krupczak KM, Post Y, Wei JJ, et al. Identification and characterization of essential genes in the human genome. Science 2015;350:1096–101 [PubMed: 26472758]
23. Christofk HR, Vander Heiden MG, Harris MH, Ramanathan A, Gerszten RE, Wei R, et al. The M2 splice isoform of pyruvate kinase is important for cancer metabolism and tumour growth. Nature 2008;452:230–3 [PubMed: 18337823]
24. Li X, Qian X, Peng LX, Jiang Y, Hawke DH, Zheng Y, et al. A splicing switch from ketohexokinase-C to ketohexokinase-A drives hepatocellular carcinoma formation. Nat Cell Biol 2016;18:561–71 [PubMed: 27088854]
25. Ma R, Zhang W, Tang K, Zhang H, Zhang Y, Li D, et al. Switch of glycolysis to gluconeogenesis by dexamethasone for treatment of hepatocarcinoma. Nat Commun 2013;4:2508 [PubMed: 24149070]

Statement of Significance:

A first-in-class HK2 antisense oligonucleotide suppresses HK2 expression in cell culture and in *in vivo*, presenting an effective, tolerated combination therapy for preventing progression of $HK1^{-}HK2^{+}$ MM tumors.

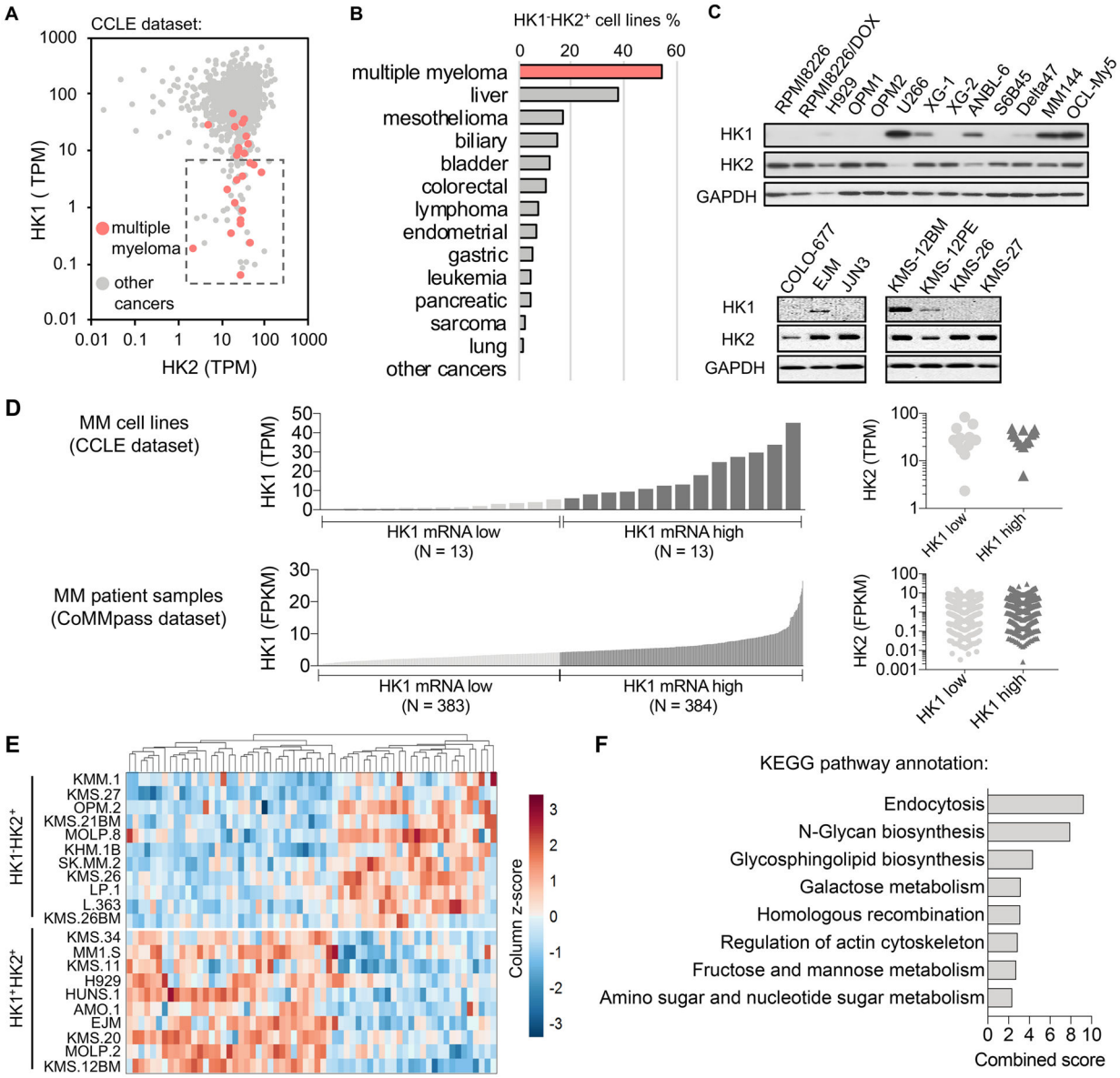

Fig. 1.

A subset of human MM cell lines are HK1^{-}HK2^{+}. (A) HK1^{-}HK2^{+} MM cell lines are present in the CCLE collection (http://oasis-genomics.org). HK1 and HK2 mRNA expression of 935 cancer cell lines, including 26 MM cell lines, are shown. Each data point represents a cell line. The box indicates "HK1^{-}HK2^{+}" cell lines, defined as HK2 > 1 TPM and HK1 < 10 TPM. TPM, transcripts per million. (B) MM has the largest percentage of HK1^{-}HK2^{+} cell lines among all CCLE cancers from different tissues of origin. (C) Validation of HK1 and HK2 protein levels in representative human MM cell lines. (D) A comparison of HK1 and HK2 expression profiles between MM cell lines (CCLE) and MM patient samples (the CoMMpass RNA-Seq datasets). (E) Differential gene expression profiles of HK1^{-}HK2^{+} and HK1^{+}HK2^{+} MM cell lines. All MM cell lines in the CCLE dataset were analyzed for differential gene expression across 18,920 genes. 63 genes with significant differences (adjusted P < 0.05) between the two populations are shown. (F)

Pathway enrichment analysis of differentially expressed genes in panel E (http://amp.pharm.mssm.edu/Enrichr/).

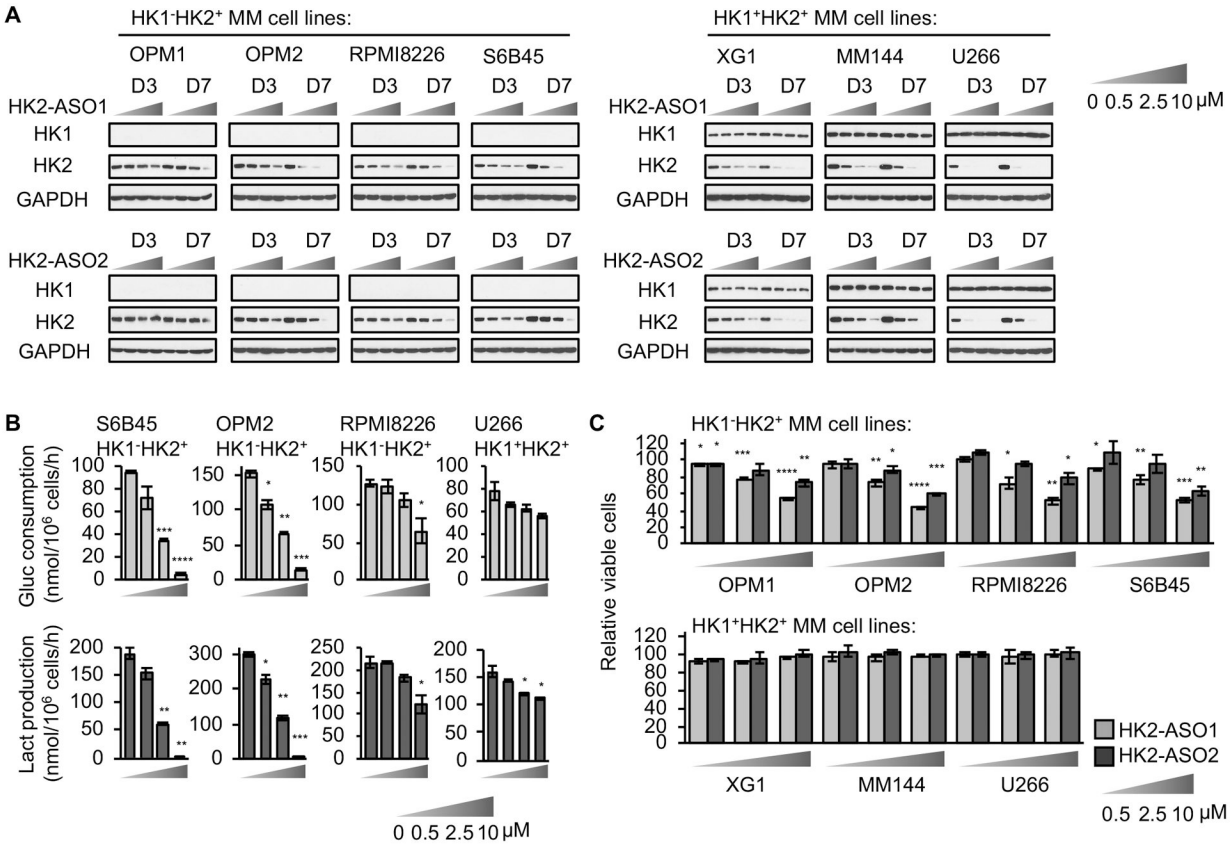

Fig. 2.

Development of human HK2 targeting ASOs. (A) HK2-ASO1 and HK2-ASO2 suppress HK2 expression in a panel of $HK1^{-}HK2^{+}$ and $HK1^{+}HK2^{+}$ MM cell lines. Cells were treated with HK2-ASO1 or HK2-ASO2 at indicated concentrations for 3 or 7 days. Cell lysates were examined for HK1 and HK2 protein levels. (B) HK2-ASO1 inhibits glucose consumption (upper panel) and lactate production (lower panel) more effectively in $HK1^{-}HK2^{+}$ MM cells than in $HK1^{+}HK2^{+}$ MM cells. Triplicate wells of cells were exposed to HK2-ASO1 for 7 days. Media were then refreshed and, after 24 h, glucose (Gluc) consumption and lactate (Lact) production were measured. (C) HK2-ASO1 and HK2-ASO2 inhibit proliferation of $HK1^{-}HK2^{+}$ MM cells but not $HK1^{+}HK2^{+}$ MM cells. Cells were treated with HK2-ASO1 or HK2-ASO2 at indicated concentrations for 7 days. Cell proliferation was measured on day 7 by MTS assays. *, $P < 0.05$. **, $P < 0.01$. ***, $P < 0.001$. ****, $P < 0.0001$.

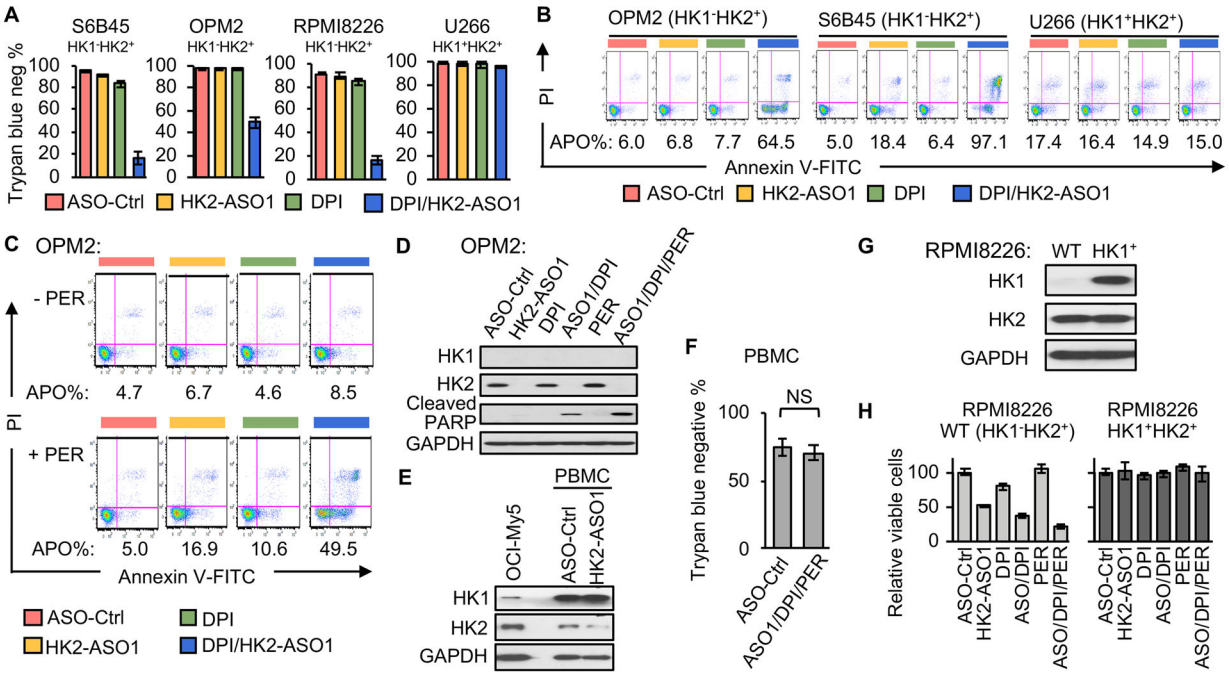

Fig. 3.

The HK2-ASO1/DPI/PER combination causes synthetic lethality in HK1^{-}HK2^{+} MM cells. (A) The combination of HK2-ASO1 and DPI causes selective synthetic lethality in HK1^{-}HK2^{+} MM cells. Cells were pre-treated with ASOs (10 μM) for 3 days, followed by the addition of DPI (50 nM) for another 3 days. Cell viability was determined by trypan blue staining. (B) The combination of HK2-ASO1 and DPI causes selective apoptosis in HK1^{-}HK2^{+} MM cells. Cells were pre-treated with ASOs (10 μM) for 3 days, followed by the addition of DPI (50 nM for OPM2 and 25 nM for S6B45 and U266) for another 3 days. Apoptosis (APO) was determined by quantification of all Annexin V-positive events. (C) PER sensitized HK1^{-}HK2^{+} OPM2 cells to apoptosis induced by the HK2-ASO1/ DPI combination. Cells were pre-treated with ASOs (5 μM) for 3 days, followed by the addition of DPI (15 nM) and PER (5 μM) for another 3 days. Apoptosis (APO) was determined by quantification of all Annexin V-positive events. (D) Effects of HK2-ASO1, DPI and PER, alone and in combination, on PARP cleavage in HK1^{-}HK2^{+} OPM2 cells. (E) Expression of HK1 and HK2 in PBMCs following treatment with 10 μM ASO-Ctrl or HK2-ASO1 for 3 days. (F) HK2-ASO1/DPI/PER combination treatment has no significant toxicity in PBMCs. PBMCs were pretreated with 10 μM ASO-Ctrl or HK2-ASO1 for 72 h, followed by the exposure to ASO-Ctrl (10 μM) or the combination HK2-ASO1(10 μM)/DPI(25 nM)/PER(5 μM) for an additional period of 72 h. Cell viability was determined by trypan blue staining in Countess II Cell counter (Invitrogen). (G) Stable expression of HK1 in RPMI8226 cells. (H) Effects of indicated treatments on cell proliferation of parental RPMI8226 (HK1^{-}HK2^{+}) and RPMI8226 (HK1^{+}HK2^{+}). Cells were exposed to ASOs (10 μM) for 72 h prior to the exposure to DPI (25 nM) and/or PER (5 μM) for another 72 h.

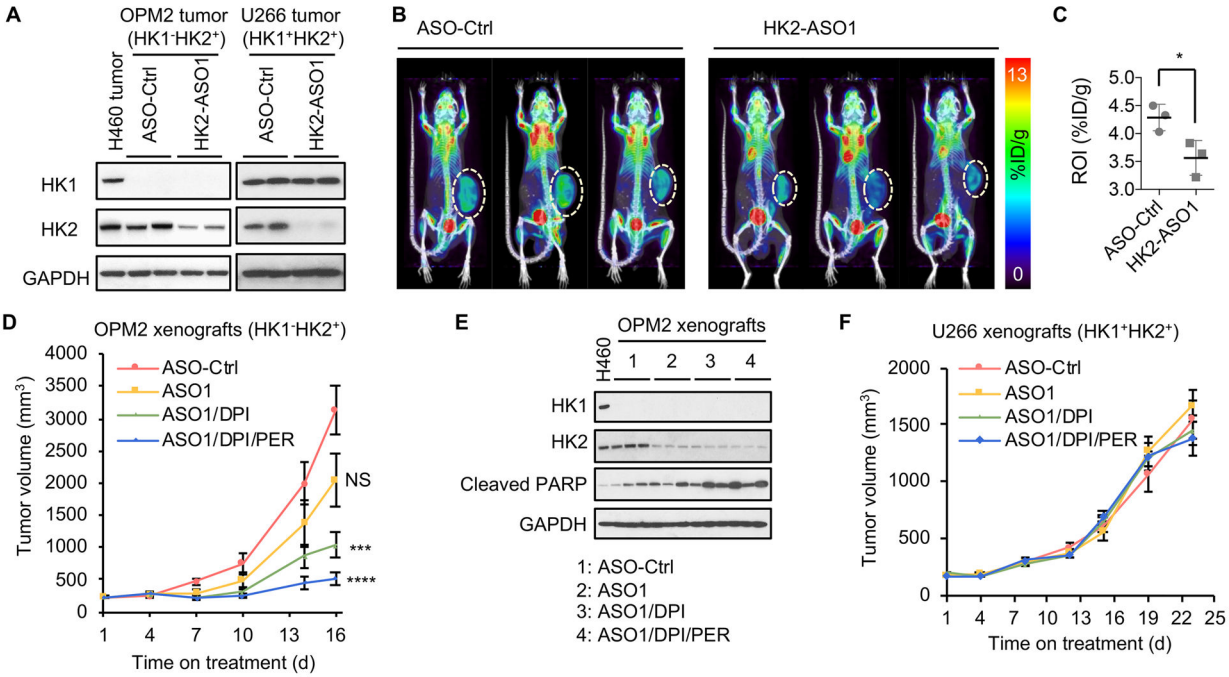

Fig. 4.

HK2-ASO1/DPI/PER combination therapy effectively suppresses $HK1^{-}HK2^{+}$ MM xenograft tumor progression. (A) HK2-ASO1 treatment suppresses HK2 expression both in xenograft $HK1^{-}HK2^{+}$ OPM2 and $HK1^{+}HK2^{+}$ U266 tumors. When xenograft tumors reached 200 mm^3, 50 mg/kg ASO-Ctrl or HK2-ASO1 were given s.c. once daily for two weeks, prior to analyses of tumor HK1 and HK2 protein expression. H460 lung cell tumor extract was used as a $HK1^{+}HK2^{+}$ control for the OPM2 samples. (B) HK2-ASO1 treatment decreases ^{18}F-FDG PET accumulation in xenograft OPM2 tumors. When xenograft tumors reached 200 mm^3, 50 mg/kg ASO-Ctrl or HK2-ASO1 was administered s.c. once daily for 10 days, prior to ^{18}F-FDG microPET imaging. (C) Quantification of PET signal in panel (B). (D) The HK2-ASO1/DPI/PER combination therapy effectively suppresses $HK1^{-}HK2^{+}$ OPM2 xenograft tumor progression. When tumors reached 200 mm^3 (day 1), xenografts were randomized into indicated groups (n = 10/group). ASO-Ctrl and HK2-ASO1 treatments started on day 1 at 50 mg/kg s.c. daily. DPI (2 mg/kg, daily i.p.) and PER (30 mg/kg, daily i.p.) started on day 3. Treatments were given for 5 days per week, with a 2-day break between weeks. (E) Treatment effects on OPM2 tumor HK1 and HK2 levels and PARP cleavage. H460 $HK1^{+}HK2^{+}$ lung cancer cell line lysate was used as a positive control for HK1 expression. (F) The HK2-ASO1/DPI/PER combination therapy has no detectable significant effect on $HK1^{+}HK2^{+}$ U266 xenograft tumor progression. N = 10/group. Treatment schedule and dosages were the same as those for OPM2 xenografts. *, $P < 0.05$. ***, $P < 0.001$. ****, $P < 0.0001$.

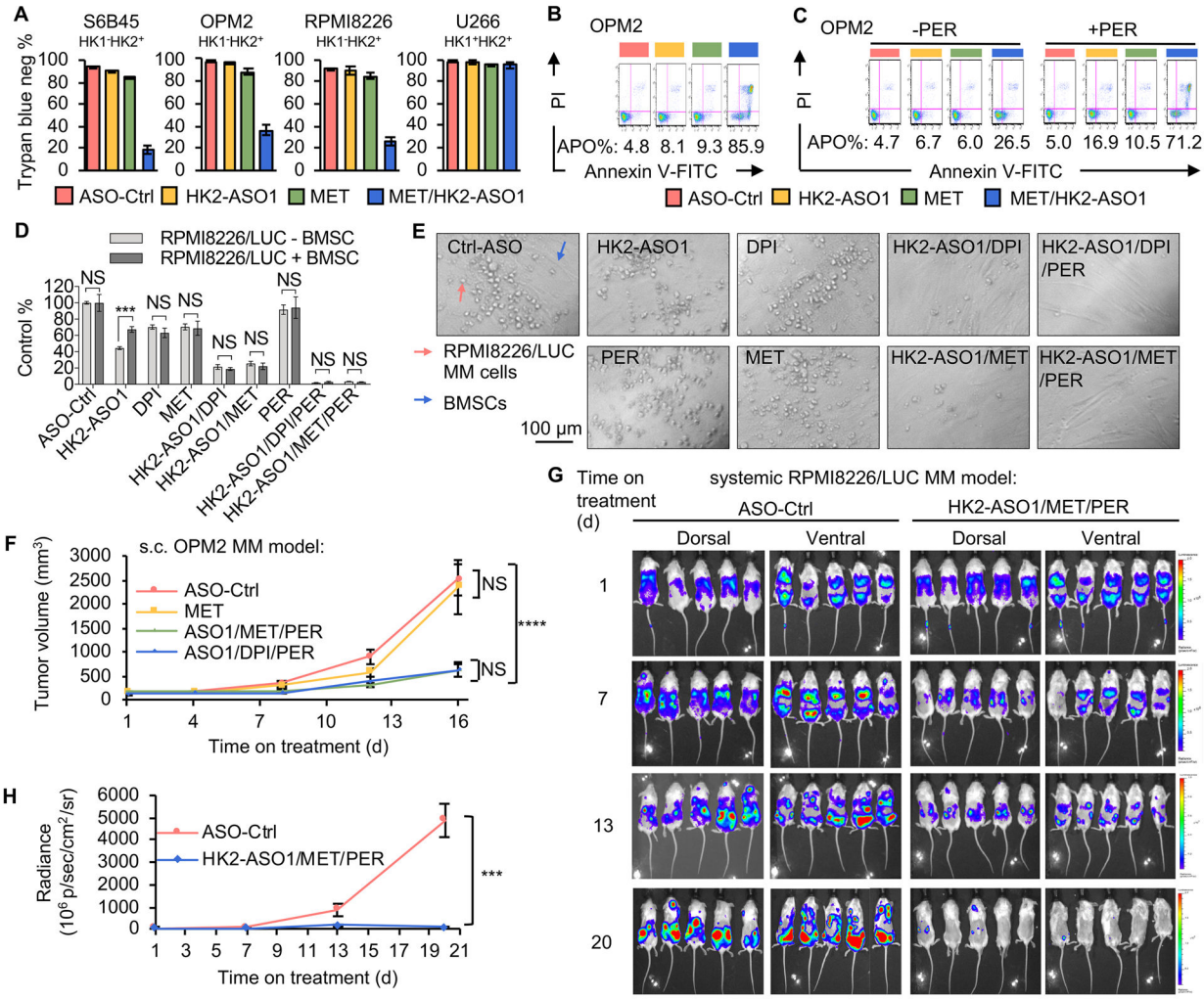

Fig. 5.

Metformin (MET) can replace DPI in the synthetically lethal combination in $HK1^{-}HK2^{+}$ MM cells. (A) The combination of HK2-ASO1 and MET causes selective synthetic lethality in $HK1^{-}HK2^{+}$ MM cells. Cells were pre-treated with HK2-ASO1 (10 μM) for 3 days, followed by the addition of MET (5 mM) for another 3 days. Cell viability was determined trypan blue staining. (B) The combination of HK2-ASO1 and MET causes selective apoptosis in OPM2 MM cells. Cells were pre-treated with HK2-ASO1 (10 μM) for 3 days, followed by the addition of MET (5 mM) for another 3 days. Apoptosis (APO) was determined by quantification of all Annexin V-positive events. (C) PER sensitized OPM2 cells to apoptosis induced by the HK2-ASO1/MET combination. Cells were pre-treated with HK2-ASO1 (5 μM) for 3 days, followed by the addition of MET (2.5 mM) and PER (5 μM) for another 3 days. Apoptosis (APO) was determined by quantification of all Annexin V-positive events. (D) Effects of single agents and combination treatments on RPMI8226/LUC cells with and without BMSC coculture. In cocultures, RPMI8226/LUC cells and BMSCs were in 1:2 ratio. Cells were exposed to 10 μM ASOs for an additional period of 3 days, prior to the exposure of 15 nM DPI, 2.5 mM MET, and/or 5 μM PER for another 3 days. RPMI8662/LUC cell proliferation was determined by measuring luminescence intensity. (E)

Representative images of co-cultures of RPMI8226/LUC and BMSCs with indicated treatments showed in panel D. (F) The combinations of HK2-ASO1/MET/PER and HK2-ASO1/DPI/PER show no demonstrably significant differences in suppressing xenograft OPM2 tumor progression. When tumors reached 200 mm^3 (day 1), xenografts were randomized into indicated groups (n = 10/group). HK2-ASO1 treatment was started on day 1 at 50 mg/kg s.c. daily. DPI (2 mg/kg, daily i.p.), MET (250 mg/kg, daily i.p.), and PER (30 mg/kg, daily i.p.) were started on day 3. Treatments were given for 5 days per week, with a 2-day break between weeks. NS, not significant. (G) Disease progression in the $HK1^{-}HK2^{+}$ RPMI8226/LUC disseminated xenograft model was monitored by BLI. BLI measurement in photons per second per cm^2 per steradian ($p/s/cm^2/sr$) was translated to color to indicate disease activity in the mice by the scales shown at far right. (H) Quantification of whole mouse BLI photons in panel G. ***, $P < 0.001$. ****, $P < 0.0001$.

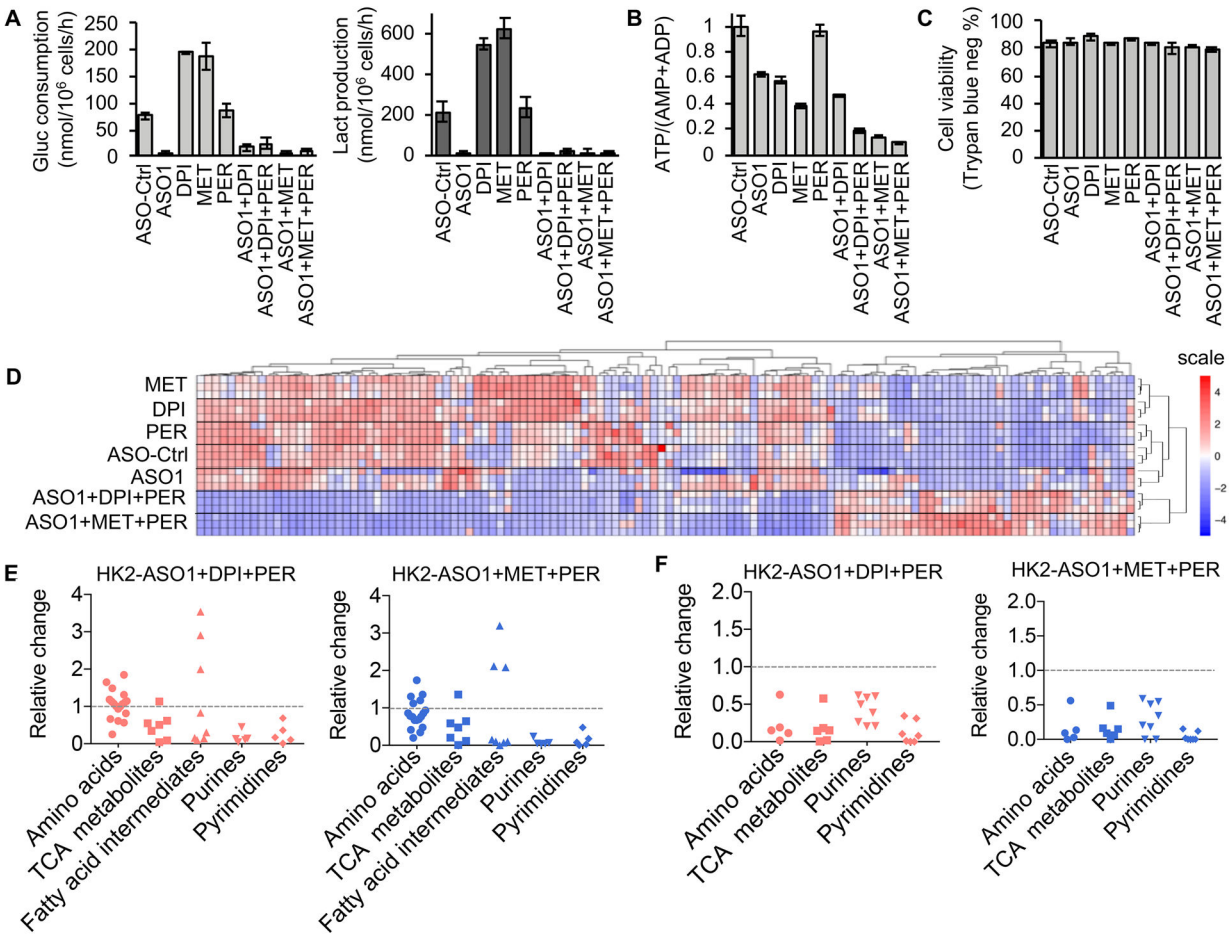

Fig. 6.

Impact of HK2-ASO1, DPI, MET, and PER on HK1^{-}HK2^{+} OPM2 cell metabolism. Effects of HK2-ASO1, DPI, MET and PER, alone and in combination for 24 h on OPM2 (A) glucose consumption and lactate production, and (B) cellular ATP/(AMP+ADP) ratios. (C) OPM2 cell viability after 24 h treatments with HK2-ASO1, DPI, MET and PER, alone and in combination, determined by trypan blue staining. No significant differences could be detected between the vehicle control and any of the experimental treatment groups. (D) Effects of HK2-ASO1, DPI, MET and PER, alone and in combination for 24 h, on the levels of 129 important metabolites in OPM2 cells. (E) Effects of 24 h treatments with HK2-ASO1/DPI/PER and HK2-ASO1/MET/PER on relative changes in cellular pool sizes of amino acids, TCA cycle metabolites, fatty acid intermediates, purines and pyrimidines in OPM2 cells. (F) Effects of 24 h treatments with HK2-ASO1/DPI/PER and HK2-ASO1/MET/PER on relative changes in ^{13}C portions of amino acids, TCA cycle metabolites, purines and pyrimidines in OPM2 cells.

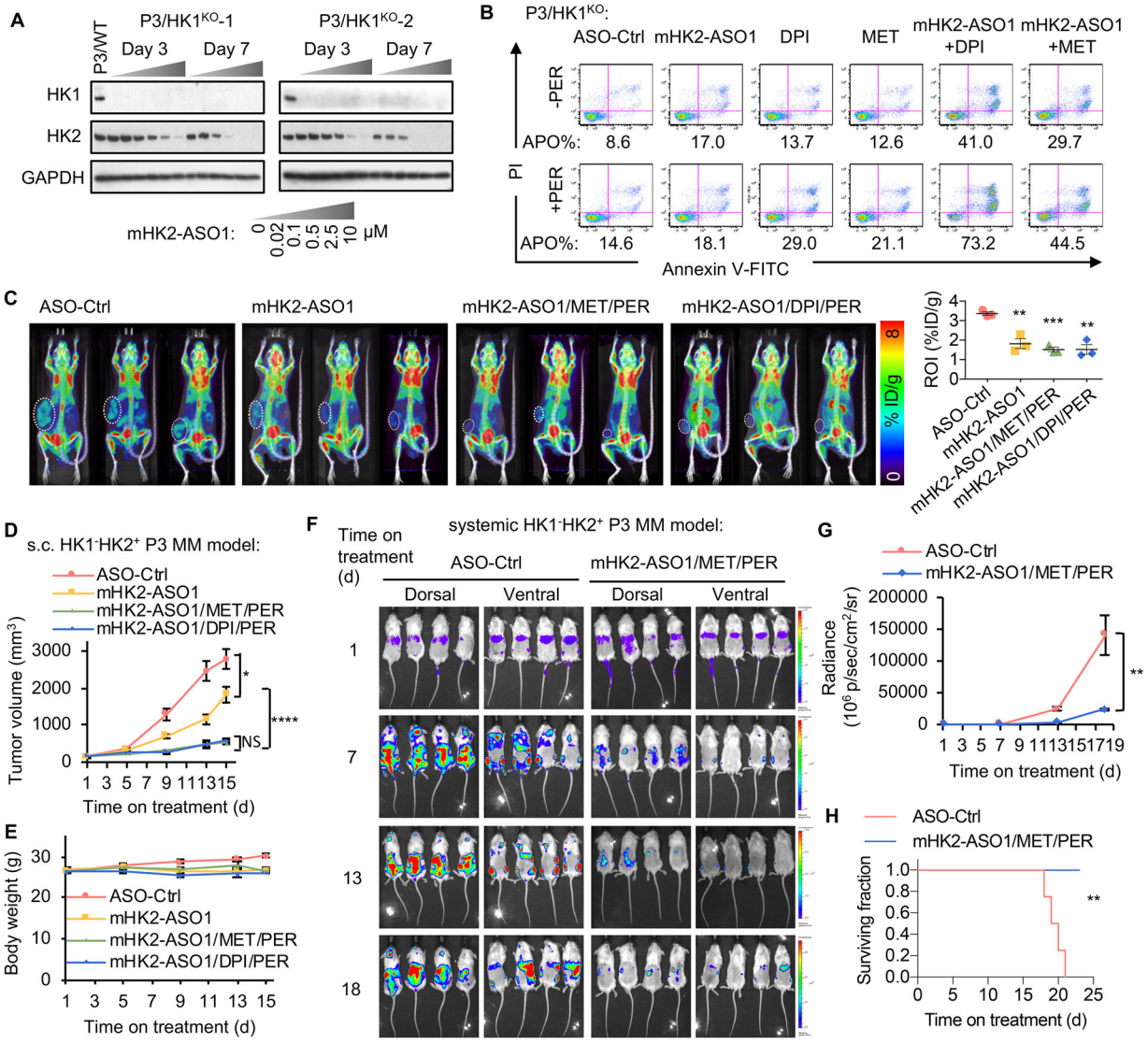

Fig. 7.

In vitro and *in vivo* effects of mouse HK2 ASOs, as single agents and in combination with DPI, MET and PER. (A) mHK2-ASO1 suppresses HK2 expression in $HK1^{-}HK2^{+}$ P3 cells. (B) The combinations of mHK2-ASO1/DPI/PER and mHK2-ASO1/MET/PER induce apoptosis in $HK1^{-}HK2^{+}$ P3 cells. Cells were pre-treated with mHK2-ASO1 (0.5 μM) for 3 days, followed by the addition of MET (2 mM), DPI (25 nM), and PER (3 μM) for another 3 days. Apoptosis (APO) was determined by quantification of the Annexin V-positive population. (C) 8-day treatments with mHK2-ASO1, mHK2-ASO1/MET/PER, and mHK2-ASO1/DPI/PER significantly reduced ^{18}F-FDG PET signal in mouse $HK1^{-}HK2^{+}$ P3 tumors. Left, PET scan images are shown. Right, quantification of PET signal intensity from tumor ROI values. (D) Effects of mHK2-ASO1, mHK2-ASO1/MET/PER, and mHK2-ASO1/DPI/PER on $HK1^{-}HK2^{+}$ P3 tumor progression. When tumors reached 200 mm^3 (day 1), mice were randomized into indicated groups (n = 11/group). mHK2-ASO1 treatment started on day 1 at 50 mg/kg s.c. daily. DPI (2 mg/kg, daily i.p.), MET (250 mg/kg, daily

i.p.), and PER (30 mg/kg, daily i.p.) started on day 3. Treatments were given for 5 days per week, with a 2-day break between weeks. NS, not significant. (E) Body weight of the four indicated groups during treatments. (F) Disease progression in the P3/HK1^{-}/mCherry-LUC disseminated model was monitored by BLI. BLI measurement in photons per second per cm^2 per steradian (p/s/cm^2/sr) was translated to color to indicate disease activity in the mice by the scales shown at far right. (G) Quantification of whole mouse BLI photons in panel F. (H) Kaplan-Meier survival curves of mice in panel F. *, $P < 0.05$. **, $P < 0.01$. ***, $P < 0.001$. ****, $P < 0.0001$.